The 9th European Congress on Computational Methods in Applied Sciences and Engineering
ECCOMAS Congress 2024
3–7 June 2024, Lisboa, Portugal

# PHASE-FIELD TOPOLOGY OPTIMIZATION OF ELASTO-PLASTIC CONTACT STRUCTURES

**ANDRZEJ M. MYŚLIŃSKI**[1]

[1]Systems Research Institute
ul. Newelska 6, 01-447 Warsaw, Poland
myslinsk@ibspan.waw.pl

**Key words:** Elasto-plasticity, contact problem, friction, topology optimization, phase-field approach.

**Summary.** The paper is concerned with the numerical solution of the topology optimization problems for elasto-plastic rather than elastic structures in unilateral frictional contact with a rigid foundation. The system of the coupled variational inequalities governs the displacement and generalized stress of this structure in contact. The material density function is the design variable. The topology optimization problem consists in finding such material distribution in the domain occupied by the body in contact to minimize the contact stress and to ensure the uniform distribution of this stress. The state system of two inequalities is approximated by the system of two nonlinear equations using the regularization technique. The phase field approach is used to approximate sharp interface problem formulation and to calculate the derivative of the cost functional. The set of necessary optimality conditions is formulated using Lagrange multiplier technique. Gradient flow equation in the form of modified Cahn-Hilliard boundary value problem is formulated and used to evaluate optimal topology domain. The examples of minimal contact stress topologies are provided and discussed.

## 1 INTRODUCTION

Topology optimization consists in material distribution within the design domain to minimize the given cost functionals describing required features of the structure [2, 6]. Most research related to topology optimization has been concerned with linear elastic structures (see references in [6]). The amount of papers dealing with non-linear elastic structures or nonlinear mechanical behavior is limited. The ability to take into account elasto-plastic materials is of great interest of industrial engineers. Plasticity models account for irreversible microscopic mechanical defects resulting in plastic areas which tend to deform more than elastic ones. This may lead either to wear and fatigue of the structure or to its damage.

The fundamentals of the theory of plasticity and elasto-plasticity, including both mechanical and mathematical aspects, are presented and discussed in many monographs [9, 17]. In the framework of theory of the variational inequalities and convex analysis the results dealing with the existence, uniqueness or regularity of solutions to these elasto-plastic material models or methods to solve them numerically are reported in these monographs. The contact problems between elasto-plastic bodies governed by variational inequalities are discussed in [7, 8]. The optimal control problems for static elasto-plastic material models with hardening have been considered in [10, 13, 18]. Since in general the solution to the state inequality is not Gâteaux

differentiable it is approximated and replaced by nonlinear equation using Huber or Moreau–Yoshida regularizations. The necessary optimality conditions have been formulated for the regularized optimal control problem and next by passing to the limit with the regularization parameter to zero the set of optimality conditions for the original control problem have been obtained. Shape or topology optimization of elasto-plastic structures have been investigated in [1, 2, 3, 12, 14, 15, 16].

The aim of this work is to solve numerically the shape and/or topology optimization problem for two bodies in contact assuming static elasto-plastic rather than elastic material model. The optimization problem consists in finding such shape of the domain occupied by the body in contact to minimize the stress along the contact boundary. It extends the previous author results from [16]. The bilateral elasto-plastic contact problem with Tresca friction is formulated using the small strain plasticity material model [5]. For the sake of the sensitivity analysis and numerical computations this problem is reformulated as dual variational problem where the displacement and the generalized stress of the body are governed by the system of two coupled variational inequalities. Using Moreau–Yosida as well as friction regularization techniques these inequalities are transformed into the set of two coupled nonlinear equations. The topology optimization problem for the bodies in contact is formulated in terms of material density function. The derivative of the cost functional is calculated and gradient flow equation formulated. The optimization problem is discretized using the finite element method. The semi-smooth Newton method is used to solve the discrete contact problem. Numerical results are reported and discussed.

## 2 CONTACT PROBLEM

Consider a body occupying a bounded domain $\Omega \subset R^d$, $d = 2, 3$, with a Lipschitz continuous boundary $\Gamma$ (see Fig. 1). The boundary $\Gamma$ is divided into three open disjoint and measurable parts $\Gamma_1$, $\Gamma_2$ and $\Gamma_3$ such that $meas(\Gamma_1) > 0$. The displacement of the body subject to deformation by a given volume force of density $\mathbf{f}_1 = \mathbf{f}_1(x)$, $x \in \Omega$, and a surface traction of density $\mathbf{f}_2 = \mathbf{f}_2(x)$ applied on the boundary $\Gamma_2$ is denoted by $\mathbf{u} = \{u_i\}_{i=1}^d$. The body is clamped along the boundary $\Gamma_1$, i.e., its displacement vanishes there. Along the boundary $\Gamma_3$ the body is assumed to be in bilateral frictional contact with the rigid foundation. The friction phenomenon is modeled by Tresca's law. The forces $\mathbf{f}_1$ and $\mathbf{f}_2$ are acting slow enough to neglect the inertial terms.

The domain $\Omega$ is filled with a material undergoing elasto-plastic deformation. In the elastic range it obeys Hooke's law [17] governed by a fourth-order tensor $\mathbb{C} = (C_{ijkl}(x))$, $i, j, k, l = 1, ...d$, such that, for any symmetric matrix $\boldsymbol{\zeta}$, $\mathbb{C} : \boldsymbol{\zeta} = 2\lambda\boldsymbol{\zeta} + \mu tr(\boldsymbol{\zeta})\mathbf{I}_d$. $\lambda$ and $\mu$ are the Lamé constants. For $\mu > 0$ and $d\lambda + 2\mu > 0$ and for almost all $x \in \Omega$ the elasticity tensor $\mathbb{C}(x)$ is symmetric, uniformly bounded and coercive [9]. Tensor $\mathbb{C} = \mathbb{C}(\rho)$ depends on material density function $\rho \in L^\infty(\Omega)$. Let us also introduce the Cauchy stress tensor $\boldsymbol{\sigma} = \sigma(\mathbf{u}) = \{\sigma_{ij}\}_{i,j=1}^d$, and the linearized strain tensor $\epsilon = \epsilon(\mathbf{u}) = \epsilon(\mathbf{u}) = \frac{1}{2}(u_{i,j} + u_{j,i})$, [17], $u_{i,j} = \frac{\partial u_i}{\partial x_j}$, $i, j = 1, ..., d$. The summation convention over repeated indices [17] is used throughout the paper. The divergence operator $\mathrm{div}(\boldsymbol{\sigma})$ of second order tensor $\boldsymbol{\sigma}$ is defined as $\mathrm{div}(\boldsymbol{\sigma}) = \{\sigma_{ij,j}\}$, $\sigma_{ij,j} = \frac{\partial \sigma_{ij}}{\partial x_j}$, $i, j = 1, ..., d$. We assume the plastic deformation of the material is governed by the additive small strain plasticity model [9, 17]. In this model the material strain $\epsilon$ is sum of the elastic strain $\epsilon^e$ and the plastic strain $\epsilon^p$, i.e., $\epsilon(\mathbf{u}) = \epsilon^e(\mathbf{u}) + \epsilon^p(\mathbf{u})$, and the stress tensor satisfies $\sigma(\mathbf{u}) = \mathbb{C} : \epsilon^e(\mathbf{u}) = \mathbb{C} : (\epsilon(\mathbf{u}) - \epsilon^p(\mathbf{u}))$,

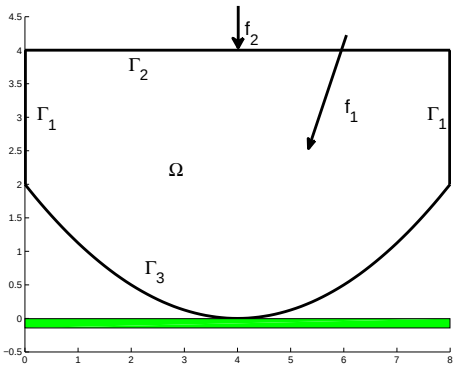


**Figure 1**: The body $\Omega$ in contact.

and $\epsilon(\mathbf{u}) = \mathbb{C}^{-1} : \sigma(\mathbf{u}) + \epsilon^p(\mathbf{u})$.

Under the loading of volume or boundary forces $\mathbf{f}_1$ and $\mathbf{f}_2$ the body material undergoes the deformation. The plastic deformation with the hardening phenomenon is governed by the generalized plastic strain $(\boldsymbol{\epsilon}^p, \boldsymbol{\xi})$ and the generalized stresses $(\boldsymbol{\sigma}, \boldsymbol{\chi})$. The back stress $\boldsymbol{\chi}$ and the internal variable $\boldsymbol{\xi}$ are related by [9] $\boldsymbol{\chi} = -\mathbb{H} : \boldsymbol{\xi}$ in $\Omega$, where $\mathbb{H} = \mathbb{H}(\rho)$ denotes the hardening tensor. The generalized plastic stress may take values only in a closed convex set $\mathcal{K}$ of admissible generalized stresses. For a given yield function $\varphi$ this set is defined as [9]

$$\mathcal{K} = \{(\boldsymbol{\sigma}, \boldsymbol{\chi}) : \ \varphi(\boldsymbol{\sigma}, \boldsymbol{\chi}) \leq 0\}. \tag{1}$$

The evolution of the plastic strain $\boldsymbol{\epsilon}^p$ and the internal variable $\boldsymbol{\xi}$ is governed by the flow rule [9, 13] described using maximal plastic work principle for the generalized stresses:

$$\begin{aligned} &\epsilon(\mathbf{u}(x)) : \boldsymbol{\sigma}(x) - \boldsymbol{\sigma}(x) : \mathbb{C}^{-1} : \boldsymbol{\sigma}(x) - \boldsymbol{\chi}(x) : \mathbb{H}^{-1} : \boldsymbol{\chi}(x) = \\ &\max_{(\mathbf{q},\boldsymbol{\eta})\in\mathcal{K}} \{\epsilon(\mathbf{u}(x)) : \boldsymbol{\sigma}(x) - \boldsymbol{\sigma}(x) : \mathbb{C}^{-1} : \mathbf{q}(x) - \boldsymbol{\chi}(x) : \mathbb{H}^{-1} : \boldsymbol{\eta}(x)\}. \end{aligned} \tag{2}$$

We shall consider the following contact problem: find the generalized stress field $(\boldsymbol{\sigma}, \boldsymbol{\chi}) : \Omega \to R^{d\times d} \times R^{d\times d}$, the displacement field $\mathbf{u} : \Omega \to R^d$, the generalized strain field $(\boldsymbol{\epsilon}^p, \boldsymbol{\xi}) : \Omega \to R^{d\times d} \times R^{d\times d}$ satisfying the plasticity conditions (1) - (2) as well as

$$\mathrm{div}\boldsymbol{\sigma} + \mathbf{f}_1 = 0 \ \text{ in } \ \Omega, \tag{3}$$

$$\mathbf{u} = 0 \ \text{ on } \ \Gamma_1 \ \text{ and } \ \boldsymbol{\sigma}_\nu = \mathbf{f}_2 \ \text{ on } \ \Gamma_2, \tag{4}$$

$$\mathbf{u}_\nu = 0, \ \mid \boldsymbol{\sigma}_\tau \mid \leq \mu_f \tilde{p} \ \text{ on } \ \Gamma_3, \tag{5}$$

$$\mid \boldsymbol{\sigma}_\tau \mid \ < \ \mu_f \tilde{p} \ \Rightarrow \ \mathbf{u}_\tau = 0 \ \text{ on } \ \Gamma_3, \tag{6}$$

$$\mid \boldsymbol{\sigma}_\tau \mid \ = \ \mu_f \tilde{p} \ \Rightarrow \ \exists \lambda \geq 0, \ \mathbf{u}_\tau = -\lambda \boldsymbol{\sigma}_\tau \ \text{ on } \ \Gamma_3. \tag{7}$$

For the unit outward normal vector $\boldsymbol{\nu}$ to the boundary $\Gamma$ normal and tangential components of the displacement field $\mathbf{u}$ are denoted by [17] $\mathbf{u}_\nu = \mathbf{u} \cdot \boldsymbol{\nu} = u_i \cdot \nu_i$, $i = 1, ..., d$, and by $\mathbf{u}_\tau = \mathbf{u} - u_\nu \boldsymbol{\nu}$, respectively. Similarly normal and tangential components of the stress field $\boldsymbol{\sigma}$ are denoted by $\boldsymbol{\sigma}_\nu = \boldsymbol{\sigma}\nu \cdot \nu$ and by $\boldsymbol{\sigma}_\tau = \boldsymbol{\sigma}\nu - \boldsymbol{\sigma}_\nu \nu$, respectively. A real constant $\mu_f > 0$ and $\mid \cdot \mid$ denote the friction coefficient and the Euclidean norm, respectively. A real constant $\tilde{p}$ is interpreted as a

bound of normal contact stress $\boldsymbol{\sigma}_\nu$ along the boundary $\Gamma_3$ [11]. For a given $\tilde{p} \geq 0$ system (1)-(7) governs the elasto–plastic bilateral contact problem with Tresca friction.

We shall formulate elasto–plastic contact problem (1)-(7) as a dual variational or so-called forward problem. This formulation is based on the generalized stress tensor $\boldsymbol{\Sigma} = (\boldsymbol{\sigma}, \boldsymbol{\chi})$ rather than on the generalized strain tensor $(\boldsymbol{\epsilon}^p, \boldsymbol{\xi})$. Let us use von Mises yield function $\varphi_M$ as the yield function $\varphi$ in (1). Von Mises yield function $\varphi_M$ has the following form [9]

$$\varphi_M(\boldsymbol{\sigma}) = \sqrt{\boldsymbol{\sigma}^D : \boldsymbol{\sigma}^D} - \sigma_{tr} =\mid \sigma^D \mid -\sigma_{tr}. \tag{8}$$

The real constant $\sigma_{tr} > 0$ denotes the material yield stress. Therefore using (8) the set of admissible generalized stresses (1) takes the form

$$\mathcal{K}_M = \{(\boldsymbol{\tau}, \boldsymbol{\eta}) \in R^{d\times d}_{sym} \times R^{d\times d}_{sym} : \mid \boldsymbol{\tau}^D + \boldsymbol{\eta}^D \mid -k_2\gamma \leq \sigma_{tr}\}, \tag{9}$$

where $k_2 \geq 0$ is the isotropic hardening parameter and $\gamma$ is a scalar determining expansion of the yield surface in the isotropic hardening or equivalent plastic strain [9]. For the sake of simplicity we assume linear hardening only, i.e., $k_2 = 0$. We denote by $W$ and $S$ the space for displacements and the space for stresses as well as back stresses, respectively:

$$W = \{\mathbf{u} \in H^1(\Omega; R^d) : \ \mathbf{u} = 0 \ \text{ on } \ \Gamma_1\} \ \text{ and } \ S = L^2(\Omega; R^{d\times d}_{sym}). \tag{10}$$

The sets of admissible displacements and admissible generalized stresses are denoted by

$$K_C = \{\mathbf{u} \in W : \ \mathbf{u}_\nu = 0 \ \text{ on } \ \Gamma_3\} \ \text{ and } \ K_M = \{(\boldsymbol{\tau}, \boldsymbol{\eta}) \in S \times S : (\boldsymbol{\tau}(x), \boldsymbol{\eta}(x)) \in \mathcal{K}_M\}. \tag{11}$$

The dual formulation of the contact problem (1)-(7) consists in the minimization of the dual energy functional [9, 13] with respect to the generalized stress $\boldsymbol{\Sigma}$. Let us define the weak solution of the contact problem (1)-(7) obtained by its formal integration by parts. An element $(\boldsymbol{\Sigma}, \mathbf{u}) = (\boldsymbol{\sigma}, \boldsymbol{\chi}, \mathbf{u}) \in S \times S \times W$ is called a weak solution of (1)-(7) if $\boldsymbol{\Sigma} \in K_M$ and $\mathbf{u} \in K_C$ as well as

$$\int_\Omega \boldsymbol{\sigma} : \mathbb{C}^{-1} : (\boldsymbol{\tau} - \boldsymbol{\sigma})dx + \int_\Omega \boldsymbol{\chi} : \mathbb{H}^{-1} : (\boldsymbol{\eta} - \boldsymbol{\chi})dx - \int_\Omega (\boldsymbol{\tau} - \boldsymbol{\sigma}) : \epsilon(\mathbf{u})dx \geq 0 \quad \forall \quad \mathbf{T} = (\boldsymbol{\tau}, \boldsymbol{\eta}) \in K_M, \tag{12}$$

$$\int_\Omega \boldsymbol{\sigma} : \epsilon(\mathbf{v} - \mathbf{u}) + \int_{\Gamma_3} \mu_f \tilde{p} \mid \mathbf{v}_\tau \mid ds - \int_{\Gamma_3} \mu_f \tilde{p} \mid \mathbf{u}_\tau \mid ds \geq \int_\Omega \mathbf{f}_1 \cdot (\mathbf{v} - \mathbf{u}))dx + \int_{\Gamma_2} \mathbf{f}_2(\mathbf{v} - \mathbf{u}) \ \forall \, \mathbf{v} \in K_C. \tag{13}$$

The elasto-plastic contact problem is governed by the system of coupled variational inequalities (12)-(13). In order to solve it numerically we transform it into the system of coupled nonlinear equations using penalization and regularization techniques. Remark, the first two terms of the inequality (12) describe the projection of the generalized stress tensor $\boldsymbol{\Sigma}$ on the admissible set $K_M$ [15]. Using the orthogonal projection operator $P_{K_M}$ of the generalized stress $\boldsymbol{\Sigma}$ on the set $K_M$ with respect to the scalar product in $S \times S$ we define a relaxed version of the optimization problem associated with (12)-(13) depending on penalty parameter $\tilde{\alpha}$. It is equivalent Moreau-Yosida approximation of the indicator function of the set $K_M$ of the admissible generalized

stresses. Recall from [9] for von Mises yield function (8) the projection operator $P_{K_M}(\boldsymbol{\Sigma})$ of tensor $\boldsymbol{\Sigma}$ on the set $K_M$ at the admissible generalized stresses is equal to

$$P_{K_M}(\boldsymbol{\Sigma}) = \boldsymbol{\Sigma} - \frac{1}{2}\max\left(0, \mid \boldsymbol{\sigma}^D + \boldsymbol{\chi}^D \mid -\sigma_{tr}\right) \frac{1}{\mid \boldsymbol{\sigma}^D + \boldsymbol{\chi}^D \mid} \begin{pmatrix} \boldsymbol{\sigma}^D + \boldsymbol{\chi}^D \\ \boldsymbol{\sigma}^D + \boldsymbol{\chi}^D \end{pmatrix}. \tag{14}$$

Since the mapping $x \to \max(0, x)$ is non-differentiable the projection operator (14) is also non-differentiable. Therefore the regularization of this projection operator consists in the regularization of the function $\max(0, \cdot)$. We denote this regularization as function $\tilde{f}_\alpha(\cdot)$ with the regularization parameter $\alpha > 0$. Function $\tilde{f}_\alpha(\cdot)$ has the form

$$\tilde{f}_\alpha(x) = \begin{cases} \frac{1}{4\alpha}x^2 + \frac{1}{2}x + \frac{\alpha}{4} & \text{for } x \in [-\alpha, \alpha], \\ \max(x, 0) & \text{otherwise.} \end{cases} \tag{15}$$

Taking into account (14) and (15) the regularized projection operator $P^\alpha_{K_M}(\boldsymbol{\Sigma})$ of the operator (14) depending on parameter $\alpha$ can be written as

$$P^\alpha_{K_M}(\boldsymbol{\Sigma}) = \boldsymbol{\Sigma} - \tilde{f}_\alpha\left(\mid \boldsymbol{\sigma}^D + \boldsymbol{\chi}^D \mid -\sigma_{tr}\right) \frac{1}{\mid \boldsymbol{\sigma}^D + \boldsymbol{\chi}^D \mid} \begin{pmatrix} \boldsymbol{\sigma}^D + \boldsymbol{\chi}^D \\ \boldsymbol{\sigma}^D + \boldsymbol{\chi}^D \end{pmatrix}. \tag{16}$$

Since the integrand function $|\cdot|: R^d \to R$ in friction term of (13) is non-smooth the inequality (13) still involves the non-differentiable term. Using the smooth function $\varphi_{\tilde{\rho}}$ depending on regularization parameter $\rho > 0$ we obtain:

$$\int_{\Gamma_3} \mu_f \tilde{p} \mid \mathbf{v}_\tau \mid ds - \int_{\Gamma_3} \mu_f \tilde{p} \mid \mathbf{u}_\tau \mid ds =$$
$$\int_{\Gamma_3} \nabla_v j_c^{\tilde{\rho}}(\mathbf{u}) v ds = \int_{\Gamma_3} \mu_f \tilde{p} \frac{d\varphi_{\tilde{\rho}}(\mathbf{u})}{du} \mathbf{v} ds \ \ \forall \mathbf{v} \in W. \tag{17}$$

For the sake of clarity let us denote by $\beta = (\tilde{\alpha}, \alpha, \tilde{\rho}) > 0$ a real regularization parameter. Using the penalization of the indicator function of the set $K_M$, as well as the regularizations (16) and (17) the original system (12)-(13) of two variational inequalities is approximated by the system of the coupled nonlinear equations: find $\mathbf{u}_\beta \in W$ and $(\boldsymbol{\sigma}_\beta, \boldsymbol{\chi}_\beta) \in S \times S$ satisfying

$$\int_\Omega \boldsymbol{\sigma}_\beta : C^{-1} : (\boldsymbol{\tau} - \boldsymbol{\sigma}_\beta) dx + \int_\Omega \boldsymbol{\chi}_\beta : H^{-1} : (\boldsymbol{\eta} - \boldsymbol{\chi}_\beta) dx -$$
$$\int_\Omega \epsilon(\mathbf{u}_\beta) : (\boldsymbol{\tau} - \boldsymbol{\sigma}_\beta) dx + \tilde{\alpha} \int_\Omega [(\sigma_\beta - P^\alpha_{K_M}(\sigma_\beta)) : (\boldsymbol{\tau} - \boldsymbol{\sigma}_\beta) +$$
$$(\boldsymbol{\chi}_\beta - P^\alpha_{K_M}(\boldsymbol{\chi}_\beta) : (\boldsymbol{\eta} - \boldsymbol{\chi}_\beta)] dx = 0 \ \ \forall\, (\boldsymbol{\tau}, \boldsymbol{\eta}) \in S \times S, \tag{18}$$
$$\int_\Omega \epsilon(\mathbf{v} - \mathbf{u}_\beta) : \boldsymbol{\sigma}_\beta(u) dx + \int_{\Gamma_3} \nabla_v j_c^\rho(\mathbf{u}_\beta)(\mathbf{v} - \mathbf{u}_\beta) ds = l(\mathbf{v} - \mathbf{u}_\beta) \ \ \forall\, \mathbf{v} \in W. \tag{19}$$

## 3 TOPOLOGY OPTIMIZATION PROBLEMS

Let us formulate the topology optimization problem for the state system (18)-(19). Topology optimization of structures consists in the determining of the optimal distribution of the material occupying the design domain $\Omega$. The sharp-interface objective functional has the form:

$$J(E, \mathbf{u}(\rho)) = \int_E \psi(\mathbf{u}(\rho)) dx + \int_\Gamma \tilde{\psi}(\mathbf{u}(\rho)) ds + Per(E; \Omega). \tag{20}$$

The functions $\psi : R^d \to R$ and $\tilde{\psi} : R^d \to R$ depend on the solution $\mathbf{u}$ to the state system (18)-(19) and are smooth enough. In applications usually the following functions are chosen

$$\psi = 0, \quad \tilde{\psi} = \sigma_\nu(\mathbf{u}) \quad \eta_\nu(x), \quad x \in \Omega, \tag{21}$$

with an auxiliary given bounded function $\eta(x)$ and its normal component $\eta_\nu$. $\sigma_\nu$ is the normal component of the stress field $\sigma = \sigma(u)$. The other choice is

$$\psi = \max\{\sigma,\ x \in \Omega\} \ \text{ or } \ \tilde{\psi} = \sigma_\nu^p,\ p \geq 2. \tag{22}$$

In (20), the set $E \subseteq \Omega$ is finite perimeter set in $\Omega$ (see [6]). It means that the characteristic function $\mathbf{1}_E$ of the set $E$ belongs to the space of bounded variations $BV(\Omega)$. Therefore the last term in (20) is used as penalty term preferring the sets $E$ with smaller rather than larger boundary. Let us formulate topology optimization problem, with $E \in BV(\Omega)$ as the control function:

$$\textit{Find set} \quad E^\star \in U_{ad}^E \ \textit{ such that: } \ J(E^\star, \mathbf{u}^\star) = \min_{E \in U_{ad}^E} J(E, \mathbf{u}), \tag{23}$$

on the set of the admissible control functions:

$$U_{ad}^E = \{E \in BV(\Omega) : \int_\Omega d\Omega = \mathit{Vol}(\Omega) \leq \mathit{Vol}^{giv}\}. \tag{24}$$

Let us also consider a phase-field approximation of the optimization problem (23). Consider the objective functional $J_\epsilon$ assumed to depend on the material density function $\rho = \rho(x)$, $x \in \Omega$. The regularized cost functional $J_\epsilon(\rho, \mathbf{u})$ is equal to:

$$J_\epsilon(\rho, \mathbf{u}) = \int_\Omega \psi(\mathbf{u}(\rho))dx + \int_\Gamma \tilde{\psi}(\mathbf{u}(\rho))ds + G(\rho), \tag{25}$$

Sub-domains of $\Omega$ where material density $\rho \approx 0$ are interpreted as voids, i.e, as areas filled with weak material. On the other hand, sub-domains of $\Omega$ where $\rho \approx 1$ are interpreted as solid phase. So, values of function $\rho$ outside the interval $[0, 1]$ have no physically meaning. The solution $\mathbf{u}$ to the state system (18)-(19) depends on $\rho$, i.e., $\mathbf{u} = \mathbf{u}(\rho)$. The regularization term $G$ of the cost functional (25) has the form of Ginzburg-Landau free energy functional:

$$G(\rho) = \int_\Omega \psi(\rho)d\Omega, \tag{26}$$

where the integrand function $\psi$ consists from:

$$\psi(\rho) = \frac{\gamma\epsilon}{2} \mid \nabla\rho \mid^2 + \frac{\gamma}{\epsilon}\psi_B(\rho). \tag{27}$$

In (27) $\epsilon > 0$ denotes a real constant, and $\gamma > 0$ is the inter-facial energy density parameter. Double-well potential function $\psi_B(\rho)$, characterizing the two phases of domain $\Omega$, has the form

$$\psi_B(\rho) = \rho^2(1 - \rho^2). \tag{28}$$

Remark, from (28) it follows, inside domain $\Omega$ void or solid phases are preferred. Intermediate material density phases, $\rho \neq 0$ or $\rho \neq 1$ are penalized in (27). Let us formulate topology optimization problem, where $\rho$ is the control function:

$$\textit{Find function} \quad \rho^\star \in U_{ad}^\rho \ \textit{ such that:} \quad J_\epsilon(\rho^\star, \mathbf{u}^\star) = \min_{\rho \in U_{ad}^\rho} J_\epsilon(\rho, \mathbf{u}), \tag{29}$$

on the set of the admissible control functions:

$$U_{ad}^\rho = \{\rho \in H^1(\Omega; [0, 1]) \cap L^\infty(\Omega; [0, 1]) : \mathit{Vol}(\rho) \leq \mathit{Vol}^{giv}\}. \tag{30}$$

## 4 NECESSARY OPTIMALITY CONDITIONS

Let us formulate the first-order necessary optimality conditions for the regularized optimization problem (29). In order to calculate the derivative of the cost functional first we shall show the differentiability of the solution to the state system (18)-(19) with respect to the material density function $\rho$. Let $p \in (2, +\infty)$, $\mathbf{f}_1 \in L^p(\Omega; R^d)$, $\mathbf{f}_2 \in L^p(\Gamma; R^d)$ and $\beta \in (0, +\infty)$. Then the control-to state operator $S_\beta : L^\infty(\Omega) \ni \rho \to (\mathbf{u}, \boldsymbol{\sigma}, \boldsymbol{\chi}) \in W \times S \times S$ is Fréchet differentiable. Its derivative in the direction $\zeta \in L^\infty(\Omega; R^d)$ is given by:

$$\begin{aligned}
\int_\Omega \boldsymbol{\sigma}'_\beta : C^{-1} : (\boldsymbol{\tau} - \boldsymbol{\sigma}_\beta)dx + \int_\Omega \boldsymbol{\sigma}_\beta : (C^{-1})' : (\boldsymbol{\tau} - \boldsymbol{\sigma}_\beta)dx + \\
\int_\Omega \boldsymbol{\chi}'_\beta : H^{-1} : (\boldsymbol{\eta} - \boldsymbol{\chi}_\beta)dx + \int_\Omega \boldsymbol{\chi}_\beta : (H^{-1})' : (\boldsymbol{\eta} - \boldsymbol{\chi}_\beta)dx - \\
\int_\Omega \epsilon(\mathbf{u}'_\beta) : (\boldsymbol{\tau} - \boldsymbol{\sigma}_\beta)dx + \tilde{\alpha} \int_\Omega [(\sigma'_\beta - (P^\alpha_{K_M})'(\sigma_\beta)) : (\boldsymbol{\tau} - \boldsymbol{\sigma}_\beta) + \\
(\boldsymbol{\chi}'_\beta - (P^\alpha_{K_M})'(\boldsymbol{\chi}_\beta) : (\boldsymbol{\eta} - \boldsymbol{\chi}_\beta)]dx = 0 \ \ \forall\, (\boldsymbol{\tau}, \boldsymbol{\eta}) \in S \times S,
\end{aligned} \tag{31}$$

$$\int_\Omega \epsilon(\mathbf{v} - \mathbf{u}_\beta) : \boldsymbol{\sigma}'_\beta(u)dx + \int_{\Gamma_3} \nabla_v j^\rho_c(\mathbf{u}'_\beta)(\mathbf{v} - \mathbf{u}_\beta)ds = l(\mathbf{v} - \mathbf{u}_\beta) \ \ \forall\, \mathbf{v} \in W. \tag{32}$$

where $\mathbf{u}'_\beta$ denotes the derivative of $\mathbf{u}_\beta$ with respect to $\rho$. Remark, from (14) it follows that the mapping

$$\boldsymbol{\sigma}^D \to \tilde{f}_\alpha(1 - \frac{\sigma_{tr}}{\mid \boldsymbol{\sigma} \mid^D}), \tag{33}$$

is strongly differentiable from $L^{2+\bar{\delta}}$ into $L^2$ for $\bar{\delta} > 0$ and its derivative is equal to

$$\frac{d\tilde{f}_\alpha}{d\boldsymbol{\sigma}^D} = \tilde{f}'_\alpha(1 - \frac{\sigma_{tr}}{\mid \boldsymbol{\sigma}^D \mid})\frac{\sigma_{tr}}{\mid \boldsymbol{\sigma}^D \mid^3}\boldsymbol{\sigma}^D. \tag{34}$$

Let us introduce the adjoint state $(z, p, q) \in W \times S \times S$ associated with the optimization problem (29). It satisfies the system of the following equations:

$$\begin{aligned}
\int_\Omega \frac{d\psi(\mathbf{u}_\beta)}{d\mathbf{u}_\beta} v dx + \int_\Gamma \frac{d\tilde{\psi}(\mathbf{u}_\beta)}{d\mathbf{u}_\beta} v ds - \int_\Omega \epsilon(\boldsymbol{v}_\beta) : (p - \boldsymbol{\sigma}_\beta)dx + \\
\int_{\Gamma_3} \nabla_v j^\rho_c(\mathbf{v}_\beta) z ds = 0 \ \ \forall \mathbf{v} \in W,
\end{aligned} \tag{35}$$

as well as

$$\begin{aligned}
\int_\Omega \boldsymbol{\tau}_\beta : \mathbb{C}^{-1}(p - \boldsymbol{\tau}_\beta)dx + \int_\Omega \boldsymbol{\eta}_\beta : \mathbb{H}^{-1}(q - \boldsymbol{\eta}_\beta)dx \\
+\tilde{\alpha} \int_\Omega [(\boldsymbol{\tau}_\beta - P'_{K_M}(\boldsymbol{\tau}_\beta)) : p + (\boldsymbol{\eta}_\beta - P'_{K_M}(\boldsymbol{\eta}_\beta)) : q]dx + \\
\int_\Omega \epsilon(z - \mathbf{u}_\beta) : \boldsymbol{\tau}_\beta(u)dx = 0 \ \ \forall (\boldsymbol{\tau}_\beta, \boldsymbol{\eta}_\beta) \in S \times S.
\end{aligned} \tag{36}$$

From (18)-(19), (31)-(32), and (35)-(36), by standard arguments [6], it follows:

**Theorem 4.1.** *The derivative $J'_\epsilon(\rho)$ of the functional (29) with respect to $\rho \in L^\infty(\Omega;\, [0,1])$ has the form:*

$$(J'_\epsilon(\rho), \zeta) = \int_\Omega \varphi_E \zeta dx, \quad \forall \zeta \in L^\infty(\Omega), \tag{37}$$

*where*

$$\varphi_E = \boldsymbol{\sigma} : (\mathbb{C}^{-1})' : p + \boldsymbol{\chi} : (\mathbb{H}^{-1})' : q + \gamma\epsilon \mid \triangle\rho \mid + \frac{\gamma}{\epsilon}\psi'_B(\rho). \tag{38}$$

If $\rho^\star \in U^\rho_{ad}$ is optimal solution to the optimization problem (29), then

$$J'_\epsilon(\rho^\star)(\rho - \rho^\star) \geq 0 \;\; \forall \rho \in U^\rho_{ad}. \tag{39}$$

## 5 NUMERICAL METHOD

In order to find the optimal material density function $\rho^\star$ and optimal topology domain $\Omega^\star$ we shall use the gradient flow rather than the optimality condition approach. Let us introduce an artificial time variable $t$, $t \in [0, T)$, $T > 0$ is given, and assume the design parameter depends on $t$, i.e., $\rho = \rho(x, t)$. We shall aim to find a stationary function $\rho$ satisfying the gradient flow equation:

$$\frac{\rho(x,t)}{\partial t} = -\frac{\partial J_\epsilon}{\partial \rho}. \tag{40}$$

From (40) we deduce in $H^{-1}$ norm [4, 19] the modified Cahn-Hilliard equation:

$$\frac{\partial \rho}{\partial t} = \nabla \cdot (\nabla \varphi_E(\rho)) \quad \text{in } \Omega, \; \forall t \in [0, T), \tag{41}$$

$$\nabla \varphi_E(\rho) \cdot n = 0 \quad \text{on } \partial\Omega, \; \forall t \in [0, T), \tag{42}$$

$$\nabla \rho \cdot n = 0 \quad \text{on } \partial\Omega, \; \forall t \in [0, T), \tag{43}$$

$$\rho(0, x) = \rho_0(x) \quad \text{in } \Omega, \; t = 0. \tag{44}$$

For the existence and regularity of solutions to (41)-(44) see [4, 19]. We shall use the finite element method to discretize and solve numerically this system. Assuming $\mathcal{T}_h$ is a regular family of partitions of domain $\Omega$, we divide this domain into disjoint open elements $T$, i.e. $\Omega = \bigcup_{T \in \mathcal{T}_h} \bar{T}$. Denote also by $h$ the discretization parameter of domain $\Omega$, i.e., $h = \max_{T \in \mathcal{T}_h}\{diam T\}$. The finite element space is defined as set of linear functions on each element $T$,

$$D^1_h = \{\eta \in C^0(\bar{\Omega}) : \eta_{|T} \in P_1(T) \;\; \forall T \in \mathcal{T}_h\} \subset H^1(\Omega). \tag{45}$$

where $P_1(T)$ denotes polynomial of order 1 on $T$. The time derivative in (41) is approximated by forward finite difference with index $n$. So, applying the mixed finite element approach [19] the system (41)-(44) is approximated by two coupled equations:

$$(\frac{\epsilon}{\tau}(\rho^n_h - \rho^{n-1}_h, \eta)_h + (\nabla \varphi^n_{Eh}, \nabla \eta)_h = 0, \; \forall \eta \in D^1_h, \tag{46}$$

$$\gamma\epsilon(\nabla \rho^n_h, \nabla \zeta)_h + \frac{\gamma}{\epsilon}(\psi'_B(\rho^{n-1}_h) + \psi''_B(\rho^{n-1}_h)(\rho^n_h - \rho^{n-1}_h), \zeta)_h - (\sigma_h : (C^{-1})' : p_h + \chi_h : (H^{-1})' : q_h, \zeta)_h = 0. \forall \zeta \;\in D^1_h. \tag{47}$$

For the results on convergence analysis of the system (46)-(47) see [19]. This system as well as the discretized systems (18)-(19) and (35)-(36) are solved numerically using generalized Newton method [8].

## 6 NUMERICAL EXAMPLE

The topology optimization problem (29) for a body occupying two-dimensional domain $\Omega \subset R^2$ in bilateral contact with the rigid foundation has been solved numerically in Matlab environment. The objective functional (25) is chosen with the following integrand functions:

$$\psi(\mathbf{u}) = 0 \quad \text{and} \quad \tilde{\psi}(\mathbf{u}) = \boldsymbol{\sigma}_\nu(u)\boldsymbol{\phi}_\nu, \tag{48}$$

and a given auxiliary function $\boldsymbol{\phi}$. The optimization problem aims to find such optimal topology of domain $\Omega$ to ensure the minimum value of contact stress peak. Since this stress usually is high, therefore it causes wear or fatigue of the contacting interfaces of the bodies. The volume constraint is given as:

$$Vol(\mathbf{u}) = \int_\Omega dx - V_0, \tag{49}$$

where constant $V_0$ denotes the volume of the initial domain $\Omega_0$. The domain $\Omega \subset R^2$ has the following structure (see Fig. 2):

$$\Omega = \{(x_1, x_2) \in R^2 : 0 \leq x_1 \leq 8 \ \wedge \ 0 < v(x_1) \leq x_2 \leq 4\}, \tag{50}$$

where the function $v(x_1) = 0.125 \cdot (x_1 - 4)^2$. The boundary $\Gamma$ of the domain $\Omega$ is divided into three mutually disjoint pieces:

$$\Gamma_1 = \{(x_1, x_2) \in R^2 : x_1 = 0, 8 \ \wedge \ 0 < v(x_1) \leq x_2 \leq 4\},$$
$$\Gamma_2 = \{(x_1, x_2) \in R^2 : 0 \leq x_1 \leq 8 \ \wedge \ x_2 = 4\},$$
$$\Gamma_3 = \{(x_1, x_2) \in R^2 : 0 \leq x_1 \leq 8 \ \wedge \ v(x_1) = x_2\}.$$

Fig. 2 displays the initial hold-all domain $D$ occupying the rectangle $[0, 8] \times [0, 4]$. This domain is divided into $80 \times 40$ grid. The initial computational domain $D$ is assumed to consists from voids (white areas on Fig. 2) as well as solid phase. The solid phase material is characterized by Young modulus $E_1 = 21 \cdot 10^5$ MPa. The voids are assumed to be filled with the weak material characterized by Young modulus $E_2 = 0.21 \cdot 10^5$ MPa.
The other data are as follows. The Poisson's ratio is $\nu = .3$. The friction coefficient is equal to $\mu_f = 0.4$. The shear and dilation moduli are equal to $8 \cdot 10^4$ MPa and $1.1 \cdot 10^5$ MPa, respectively. The yield stress $\sigma_{tr} = 367, 4$ MPa. The hardening parameters are equal to $k_1 = 1 \cdot 10^5$ MPa and $k_2 = 0$ MPa. The body is loaded by the boundary traction $f_2 = -6.5 \cdot 10^7$ N along the boundary $\Gamma_2$. The body force $f_1 = 0$.

Fig. 3 presents the optimal domain $\Omega^\star$ obtained by solving structural optimization problem (29) in the computational domain $D$. Weak material or void phases denoted by white colour are concentrated in the central part of the domain as well as close to the clamped edges. Comparing to [18], in a case of elasto-plastic materials the mass of the structure is larger than in a case of elastic model. From Fig. 4 it results, the maximal Von Mises effective stress concentration areas appear along the contact zone (denoted by red colour). There are also large stress concentration areas close to the clamped edges. Inside the domain there are a few subareas with enhanced stress but lower than close to the contact boundary. Fig. 5 displays the obtained normal contact stress vs the initial stress along the contact boundary $\Gamma_3$. The normal contact stress for the optimal topology domain has been significantly reduced comparing to the initial one.

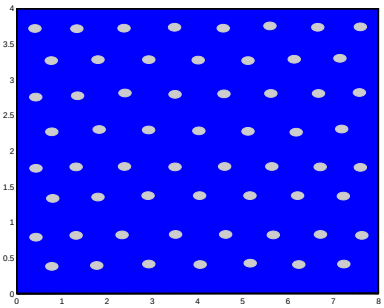

**Figure 2**: Initial computational domain $D$.

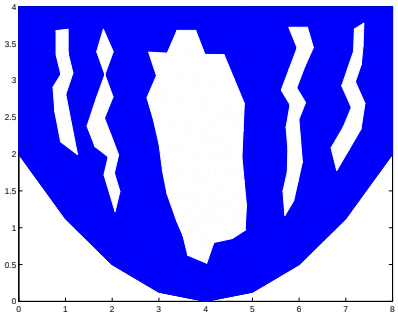

**Figure 3**: Optimal topology domain $\Omega^\star$.

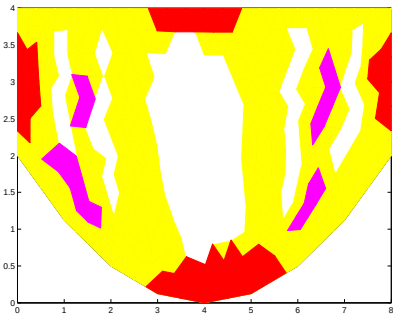

**Figure 4**: von Mises stress distribution.

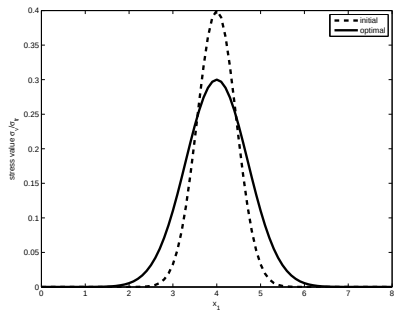


**Figure 5**: Maximal von Mises stress on the contact boundary.

## 7 CONCLUSIONS

The obtained results indicate that the application of the phase field technique allows to solve numerically a topology optimization problem for bodies in bilateral frictional contact where nonlinear small strain elasto-plastic with linear kinematic hardening material model rather than elastic material model is used. It is capable of finding topologies that generates minimum contact stress and reduce it significantly with respect to the initial topology. This approach is flexible and can be extended to solve other topology optimization problems for structures governed by nonlinear equations.

## REFERENCES

[1] S. Adly, S., Bourdin, L., Caubet, F., de Cordemoy, A.J. 2023. "Shape Optimization for Variational Inequalities: The Scalar Tresca Friction Problem." SIAM Journal on Optimization, 33(4):2512-2541.

[2] Almi, S. and Steffanelli, U. 2021. "Topology Optimization for Incremental Elastoplasticity: A Phase-Field Approach." SIAM Journal on Control and Optimization 59:339-364.

[3] Blachowski, B., Tauzowski, P., Logo, J. 2020. "Yield limited optimal topology design of elastoplastic structures." Struct. Multidisc. Optim., 61:1953-1976.

[4] Brunk, A., Egger, H., Oyedeji, T.D., Yang, Y., Xu, B.X. 2024. "On existence, uniqueness and stability of solutions to Cahn-Hilliard/Allen-Cahn systems with cross-kinetic coupling." Nonlinear Analysis: Real World Applications, 77:104051.

[5] Capatina, A., Timofte, C. 2014. "Boundary optimal control for quasistatic bilateral frictional contact problems". Nonlinear Analysis 94:84-99.

[6] Delfour, M.C., Zolesio, J.P. 2011. Shapes and Geometries: Metrics, Analysis, Differential Calculus, and Optimization, Second Edition, Advances in Design and Control series 22, SIAM.

[7] Ghaednia, H., Wang, X., Saha, S., Xu, Y., Sharma, A., Jackson, R.L. 2017. "A Review of Elastic-Plastic Contact Mechanics.", Appl. Mech. Rev 69:1-30.

[8] Hager, C., Wohlmuth, B.I. 2009. "Nonlinear complementarity functions for plasticity problems with frictional contact." Comput. Methods Appl. Mech. Engrg. 198:3411-3427.

[9] Han, W., Reddy, B.D. 2013. Plasticity. Mathematical Theory and Numerical Analysis. 2nd edition, Springer, New York.

[10] Herzog, R., Meyer, Ch. 2011. "Optimal control of static plasticity with linear kinematic hardening." Z. Angew. Math. Mech. 91:777-794.

[11] S. Kaliszky, J. Logo, T. Havady, "Optimal design of elasto-plastic structures under various loading conditions and displacement constraints." Periodica Polytechnica. Civil Engineering, 33 (1989), 107-122.

[12] Kim, N.H., Choi, K.K., and Chen, J.S. 2000. "Shape design sensitivity analysis and optimization of elasto-plasticity with frictional contact." AIAA Journal 38:1742-1753.

[13] De los Reyes, J.C., Herzog, R., and Meyer, C. 2016. "Optimal control of static elasto-plasticity in primal formulation." SIAM J. Control Optim., 54:3016-3039.

[14] Luft, D., Schulz, V., and Welker, K. 2020. "Efficient Techniques for Shape Optimization with Variational Inequalities using Adjoints." SIAM J. Optimization, 30(3):1922–1953.

[15] Maury, A., Allaire, G., Jouve, F. 2018. "Elasto-plastic shape optimization using level set method." SIAM Journal on Control and Optimization 56:556-581.

[16] Myśliński, A. "Phase Field Approach to Topology Optimization of Elasto-Plastic Contact Problems", In Nonsmooth Problems with Application in Mechanics, edited by S. Migórski and M. Sofonea, 167-189, Banach Center Publications, Vol. 127, Warsaw, Poland, ISBN 978-83-86806-57-7.

[17] Necas, J., Hlavácek, I. 2002. Mathematical Theory of Elastic and Elasto-Plastic Bodies. Elsevier.

[18] Werner, S., Stingl, M., Leugering, G. 2017. "Model-based control of dynamic frictional contact problems using the example of hot rolling." Computer Methods in Applied Mechanics and Engineering 319:442-471.

[19] Yang, J., Kim, J. 2020. "An unconditionally stable second order accurate method for systems of Cahn–Hilliard equations." Communications in Nonlinear Science and Numerical Simulation, 87:105276.